

# Calix[3]pyrrole: A Missing Link in Porphyrin-Related Chemistry

Yuya Inaba, Yu Nomata, Yuki Ide, Jenny Pirillo, Yuh Hijikata, Tomoki Yoneda, Atsuhiko Osuka, Jonathan L. Sessler,\* and Yasuhide Inokuma\*



Cite This: *J. Am. Chem. Soc.* 2021, 143, 12355–12360



Read Online

ACCESS |



Metrics & More



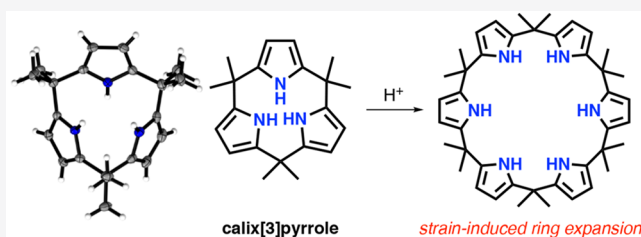
Article Recommendations



Supporting Information

**ABSTRACT:** A long-standing question in porphyrin chemistry is why pyrrole monomers selectively form tetrapyrrolic macrocycles, whereas the corresponding tripyrrolic macrocycles are never observed. Calix[3]pyrrole, a tripyrrolic porphyrinogen-like macrocycle bearing three  $sp^3$ -carbon linkages, is a missing link molecule that might hold the key to this enigma; however, it has remained elusive. Here we report the synthesis and strain-induced transformations of calix[3]pyrrole and its furan analogue, calix[3]furan. These macrocycles are readily accessed from cyclic oligoketones.

Crystallographic and theoretical analyses reveal that these three-subunit systems possess the largest strain energy among known calix[ $n$ ]-type macrocycles. The ring-strain triggers transformation of calix[3]pyrrole into first calix[6]pyrrole and then calix[4]pyrrole under porphyrin cyclization conditions. The present results help explain the absence of naturally occurring three-pyrrole macrocycles and the fact that they are not observed as products or intermediate during classic porphyrin syntheses.



## INTRODUCTION

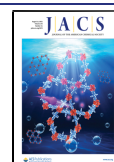
Porphyrins and related tetrapyrrole macrocycles, including heme and chlorophyll, play critical roles in biological processes as diverse as light-harvesting,<sup>1</sup> oxygen transport,<sup>2</sup> and electron transfer. They and their synthetic analogues have also attracted attention as catalysts,<sup>3,4</sup> photosensitizers,<sup>5,6</sup> and optoelectronic materials.<sup>7</sup> Because a facile one-pot synthetic procedure leading to symmetric porphyrins was reported by Rothmund in 1935,<sup>8</sup> macrocyclization of pyrrole monomers has been exhaustively examined by using various condensation conditions.<sup>9</sup> A long-standing question associated with both biological and laboratory porphyrin syntheses is why pyrrole monomers selectively form tetrapyrrolic macrocycles, whereas the corresponding tripyrrolic macrocycles are never observed. While macrocycles with five or more pyrrole units can be isolated in free form under conditions of kinetic control,<sup>10</sup> a boron template is necessary to generate and stabilize their tripyrrolic analogues.<sup>11–13</sup> It is thus not currently known whether such systems are even capable of existence. Calix[3]pyrrole, a tripyrrolic porphyrinogen-like macrocycle bearing three  $sp^3$ -carbon linkages, is a missing link molecule that might hold the key to this enigma; however, it has remained elusive. Here we report the synthesis and strain-induced transformations of calix[3]pyrrole and its furan analogue, calix[3]furan. These macrocycles are readily accessed from cyclic oligoketones. Crystallographic and theoretical analyses reveal that these three-subunit systems possess the largest strain energy among known calix[ $n$ ]-type macrocycles. The ring-strain triggers transformation of calix[3]pyrrole into first calix[6]pyrrole and then calix[4]pyrrole under porphyrin cyclization conditions. The present results help explain the

absence of naturally occurring three-pyrrole macrocycles and the fact that they are not observed as products or intermediate during classic porphyrin syntheses. Furthermore, the strain-induced ring expansion observed for calix[3]pyrrole could provide a access to new, entropically disfavored larger pyrrolic macrocycles.

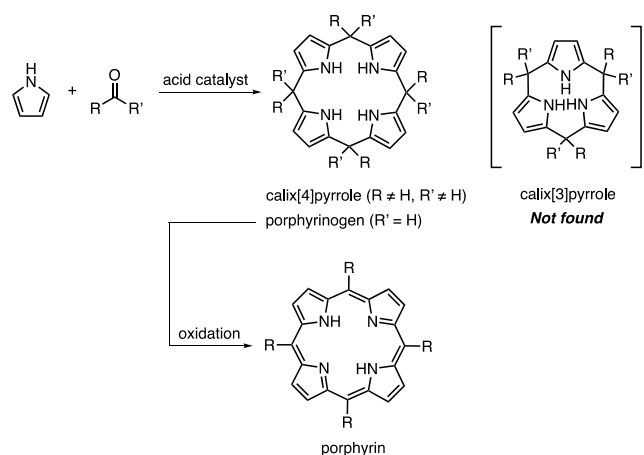
Tetrapyrrolic macrocycles are typically synthesized by linking four pyrrole monomers to furnish porphyrinogen intermediates. Porphyrinogens are macrocyclic species that possess the basic connectivity of the final porphyrin ring product but which are linked by four  $sp^3$ -hybridized *meso*-carbon atoms. In the case of porphyrinogens bearing no more than one substituent on each of the *meso*-carbons, the porphyrinogens are thermodynamically unstable under oxidizing conditions and are readily converted to the corresponding porphyrins. In contrast, porphyrinogen analogues bearing two non-hydrogen atoms on the *meso* bridges are often stable, as in the case of calix[4]pyrrole (5,10,15,20-octamethylporphyrinogen). Isolation and study of calix[3]pyrrole, the corresponding tripyrrolic macrocycle, might therefore hold the key to understanding why tripyrrolic macrocycles are not found in nature and are not observed under classic, template-free porphyrin-forming reaction conditions (Scheme 1). However, in spite of considerable synthetic effort,<sup>14,15</sup> only

Received: June 18, 2021

Published: July 28, 2021



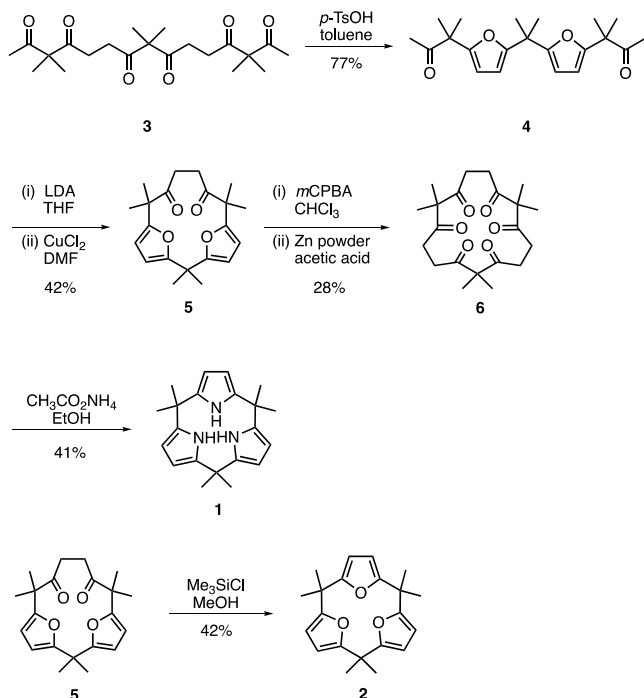
Scheme 1. A Typical Synthesis of Tetrapyrrole Macrocycles



core-modified or ring-expanded analogues of calix[3]pyrrole are known.<sup>16–19</sup> Here, we report the synthesis of calix[3]pyrrole **1** and its furan analogue calix[3]furan **2** starting from a common linear hexaketone intermediate. Both **1** and **2** undergo strain-induced transformations that provide an experimental rationale for why these elusive macrocycles have not previously been observed.

To access calix[3]pyrrole, we conceived of a synthetic route involving Paal–Knorr pyrrole ring formation from a hexaketone macrocyclic precursor (Scheme 2). A similar

Scheme 2. Synthesis of Calix[3]pyrrole and Calix[3]furan



approach proved effective for the size-selective synthesis of ring-expanded analogues, such as calix[5]pyrrole,<sup>20</sup> with the requisite cyclic oligoketone precursors being accessed from the corresponding calix[*n*]furans ( $n \geq 4$ ).<sup>21</sup> Unfortunately, calix[3]furan, the logical precursor to our targeted cyclic hexaketone intermediate, is not known. Recently we developed a synthetic strategy allowing access to aliphatic oligoketones

with precise chain lengths,<sup>22,23</sup> including the linear hexaketone **3**. Compound **3** thus became the starting point for our synthesis of **1**.

## RESULTS AND DISCUSSION

Dehydrative condensation of **3** in the presence of *p*-toluenesulfonic acid (*p*-TsOH) using a Dean–Stark trap furnished the difuran compound **4**, a linear intermediate in which the terminal carbonyl groups remain free, in 77% yield. Treatment of **4** with 3.5 equiv of lithium diisopropylamide (LDA) generated a dienolate species that underwent intramolecular cyclization upon oxidation with  $\text{CuCl}_2$  to give macrocycle **5** in 42% yield. The two furan rings in **5** were converted to the corresponding enedione units by oxidative treatment with *m*-chloroperbenzoic acid (*m*CPBA). Subsequent reduction by using zinc powder gave the cyclic hexaketone **6** in 28% yield over two steps. When the cyclic ketone **6** was subject to Paal–Knorr reaction conditions in the presence of an excess of ammonium acetate,<sup>21</sup> *meso*-hexamethylcalix[3]pyrrole **1** was obtained in 41% yield as a colorless solid. Three signals at 6.71, 5.83, and 1.59 ppm assignable to the NH, pyrrole  $\beta$ -H, and methyl protons, respectively, were seen in the proton nuclear magnetic resonance ( $^1\text{H}$ NMR) spectrum of calix[3]pyrrole **1** in  $\text{CDCl}_3$ , a finding consistent with the presence of a time-averaged  $C_{3v}$  molecular symmetry predominating in solution. A high-resolution electrospray ionization time-of-flight (ESI–TOF) mass spectrometric analysis of **1** revealed a parent ion peak at  $m/z = 320.2131$ , which was assigned to a  $[\mathbf{1}-\text{H}]^-$  molecular ion (calculated for  $\text{C}_{21}\text{H}_{26}\text{N}_3$ ,  $m/z$  320.2132).

Calix[3]furan **2** was also synthesized from cyclic difuran **5** by treating with an excess of chlorotrimethylsilane in methanol under reflux for 20 min and isolated in 42% yield.<sup>24</sup> The  $^1\text{H}$  NMR spectrum of calix[3]furan **2** also proved consistent with a  $C_{3v}$  symmetric structure. Specifically, two singlet signals at 5.80 and 1.63 ppm, assigned to the furan  $\beta$ -H and methyl protons, respectively, were seen. In the high-resolution ESI–TOF mass spectrum, peaks corresponding to a sodium adduct  $[\mathbf{2} + \text{Na}]^+$  were observed at  $m/z = 347.1615$  (simulated value for  $\text{C}_{21}\text{H}_{24}\text{O}_3\text{Na} = m/z$  347.1618).

Diffraction grade crystals of calix[3]pyrrole **1** were obtained by vapor diffusion of hexane into a dichloromethane solution in the absence of any particular effort at drying. The resulting structure (Figure 1A) revealed that two of the three pyrrolic nitrogen atoms are on the same side of the macrocycle and hydrogen-bonded to a cocrystallized water molecule (Figure S4). The distances between neighboring nitrogen atoms were in the range of 2.8573(12)–2.9701(13) Å, reflecting a relatively narrow central cavity. Notably, all three *meso*-carbon atoms were located out of the mean plane of the pyrrole rings. Distortion of the macrocycle was also observed in the crystal structure of calix[3]furan **2** (Figure 1B), although in this case a cone-shaped structure is seen in which all the furan rings point in the same direction.

The solid state structural findings are consistent with the presence of considerable strain within both calix[3]pyrrole **1** and calix[3]furan **2**. To compare the ring strains of **1** and **2** with those of larger calix[*n*]-type macrocycles, the deformation angles  $\alpha$  and  $\beta$  (Figure 1C–E), used for evaluating the displacement around aromatic units in cyclophane-type macrocycle,<sup>25</sup> were derived from the respective crystal structures. The  $\alpha$  angles of **1** and **2** were 2.52° and 1.95°, respectively. These angles are larger than those of typical

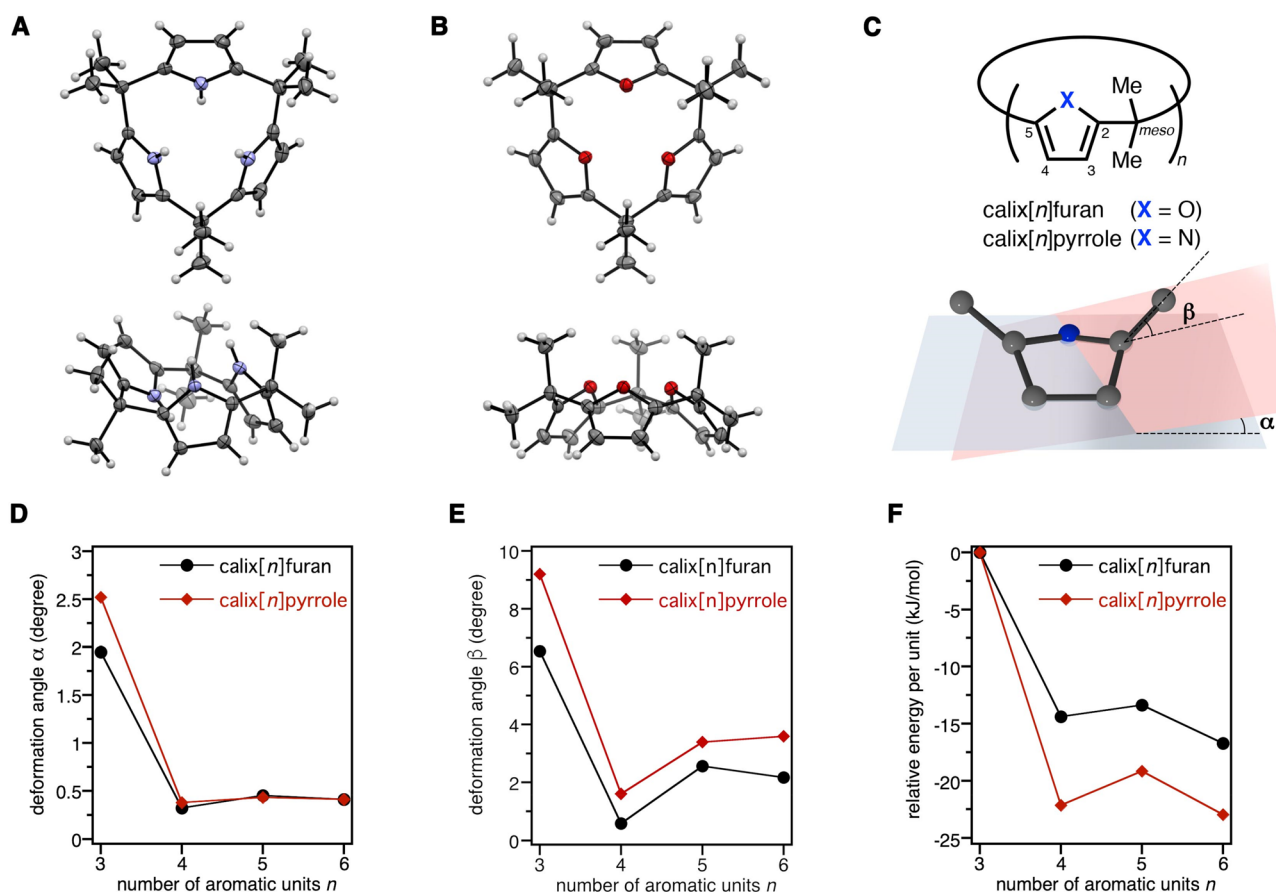


**Figure 1.** (A, B) ORTEP drawings of crystal structures of **1** and **2** at the 50% thermal probability level (top: top view; bottom: side view). Hydrogen: white; carbon: gray; nitrogen: light blue; oxygen: red. Solvent molecules are omitted for clarity. (C) Definitions of deformation angles  $\alpha$  and  $\beta$  for calix[ $n$ ]-type macrocycles.  $\alpha$  is the averaged deviation angle between mean planes of X-C(3)-C(4) (shown as light blue) and X-C(2)-C(3) (shown as light red).  $\beta$  is the averaged deviation angle between the mean plane X-C(2)-C(3) and a C(2)-C(meso) bond. (D) Deformation angles  $\alpha$  determined from crystal structures of calix[ $n$ ]pyrroles and furans ( $n = 3-6$ ). (E) Deformation angles  $\beta$  determined from these same crystal structures. (F) Calculated energy per repeat unit of calix[ $n$ ]furans and calix[ $n$ ]pyrroles relative to those for  $n = 3$  (compounds **1** and **2** of this study) at the B3LYP/cc-pVTZ level of theory.

calix[ $n$ ]pyrroles and furans ( $n = 4-6$ ), for which values of  $0.32^\circ-0.43^\circ$  are seen, and thus taken as evidence of strain. The  $\beta$  angles for **1** and **2** were found to be >2-fold greater than those of the corresponding larger macrocycles; this is reflective of a large displacement of the meso-carbon atoms from the mean plane of the neighboring aromatic rings.

Theoretical calculations provided support for the large strain energy inferred for macrocycles **1** and **2** (Figure 1F). The relative energies of the monomeric subunits in each calix[ $n$ ]-type macrocycle were calculated at the B3LYP/cc-pVTZ level by using a Grimme-type dispersion correction by optimization of the geometries using the crystal structures as the initial inputs. Compared with the corresponding calix[4]-type macrocycles, calix[3]pyrrole **1** and calix[3]furan **2** were found to be unstable by 22.1 and 14.4 kJ/mol per repeat unit, respectively. Such a large energy difference helps rationalize why calix[3]-type macrocycles are not observed during the formation of tetrapyrrolic macrocycles under equilibrium conditions.

The large ring strain of **1** was expected to lead to rapid ring expansion under standard pyrrole macrocyclization conditions.<sup>26-28</sup> To test this hypothesis, calix[3]pyrrole **1** was dissolved in dichloromethane in the presence of trifluoroacetic acid (TFA, 10 mmol/L) at room temperature, and the reaction was monitored by  $^1\text{H}$  NMR spectroscopy (Figure 2). The

signal intensity of **1** decreased by >75% within 5 s and completely disappeared after 30 s concurrent with the appearance of an intense peak ascribed to the pyrrole  $\beta$ -H of calix[6]pyrrole **7** at 5.81 ppm along with several minor peaks (Figure 2B).<sup>21</sup> ESI-TOF mass spectrometric analysis of the reaction mixture at early times revealed a parent ion peak for [7-H] $^-$  at  $m/z = 641.4340$  (calculated for  $\text{C}_{42}\text{H}_{53}\text{N}_6$   $m/z$  641.4337). The intensity of the peak attributed to hexapyrrole **7** was then seen to decrease gradually over the course of  $\sim 4$  h while new signals, corresponding to calix[4]pyrrole **8**, were seen to increase. Eventually, the  $^1\text{H}$  NMR signals converged to those of **8** (80% NMR yield). The stability of **1** was also tested under standard calix[4]pyrrole-forming conditions (i.e., catalytic HCl in ethanol).<sup>26</sup> Again, ring expansion was seen (Figure S11). While the conversion of expanded porphyrinogens into tetrapyrrole macrocycles (ring contraction) is entropically favorable and has been observed under acidic equilibrium conditions,<sup>29</sup> the formation of larger macrocycles from a smaller analogue is entropically unfavorable. The initial formation of hexapyrrole **7** from **1** is thus attributable to the strain-induced macrocyclic ring cleavage of **1** and a subsequent dimerization to give a less-strained species (i.e., **7**). The rapidity of this ring expansion reaction leads us to suggest that even were initial cyclotrimerization to occur when pyrroles

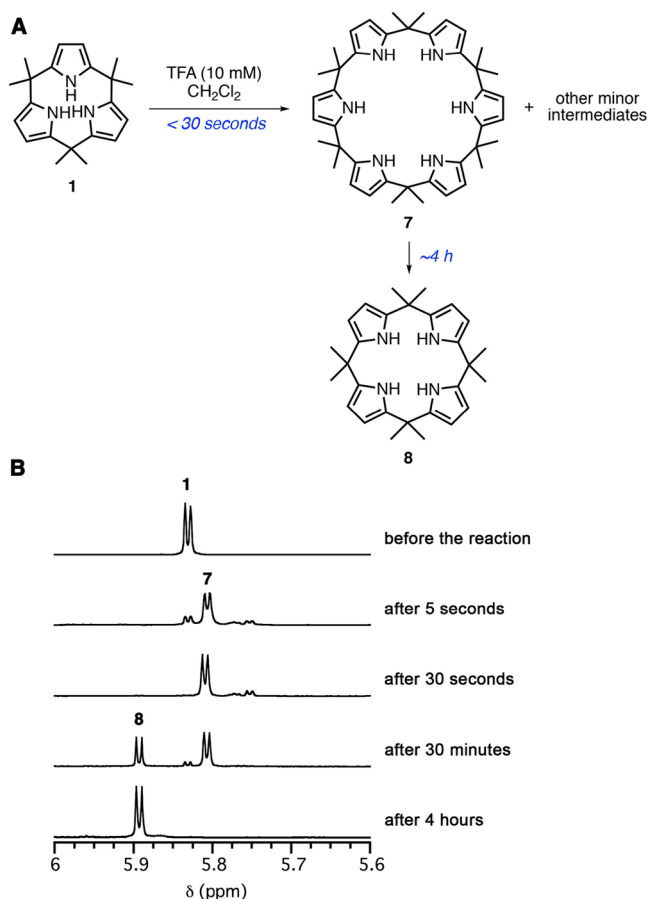
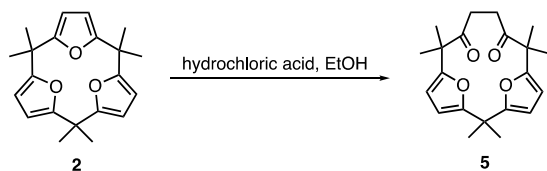


**Figure 2.** (A) Strain-induced ring-expansion reaction of calix[3]pyrrole **1** in the presence of TFA. (B) 400 MHz  $^1\text{H}$  NMR spectra monitoring of the ring-expansion reaction of **1** in a 10 mM dichloromethane solution of TFA at room temperature. All the spectra were recorded in  $\text{CDCl}_3$  after quenching the reaction by washing with aqueous sodium bicarbonate solution, drying over anhydrous magnesium sulfate, and evaporation of the solvent.

monomers are subject to acid catalyzed condensation, no calix[3]pyrrole-type products would be observed.

Unlike calix[3]pyrrole **1**, calix[3]furan **2** underwent a strain-induced ring-opening of the furan component (Scheme 3).

### Scheme 3. Strain-Induced Reaction of Calix[3]furan



Under the macrocyclization conditions optimized for calix[4]furan formation (i.e., ethanol, 12 M HCl (v/v, 2:1)),<sup>30</sup> one of the furan subunits of calix[3]furan **2** was seen to undergo hydrolysis to give diketone **5** in near-quantitative yield (Figure S12). Such a hydrolysis reaction was not observed for calix[4]furan under the same conditions. This disparity is again ascribed to differences in ring strain for calix[3]pyrrole vs calix[4]furan.

We next examined whether calix[3]pyrrole **1** could be stabilized by chemical means (Figure 3). Calix[ $n$ ]pyrroles ( $n \geq 4$ ) are known to bind Lewis basic anions via formation of

pyrrole NH-anion hydrogen-bonded complexes. Typically, this results in stabilization of specific conformations.<sup>31</sup> When tetrabutylammonium fluoride (TBAF) was titrated into a 10.0 mM  $\text{CD}_2\text{Cl}_2$  solution of **1**, the NH proton signal at 6.91 ppm in the  $^1\text{H}$  NMR spectrum was seen to shift to lower field in a concentration-dependent manner. Job's plot and curve fittings of the NMR titration results proved consistent with the formation of a 1:1 complex between **1** and the fluoride anion with an association constant of  $230 \pm 20 \text{ M}^{-1}$ . This value is much smaller than that seen for calix[4]pyrrole **8** ( $17170 \pm 900 \text{ M}^{-1}$ ).<sup>31</sup> The association constants corresponding to the interaction of calix[3]pyrrole **1** with other halide anions were  $\leq 10 \text{ M}^{-1}$ . The fluoride complex  $\mathbf{1}\cdot\text{F}^-$  could be crystallized by slow evaporation of a dichloromethane solution. The resulting crystal structure revealed a cone-shaped conformation for **1** to which a fluoride ion was hydrogen bonded via all three NH protons with N–F distances of 2.681(2), 2.683(2), and 2.736(2) Å (Figure 3B). The distance from the fluoride ion to the mean plane of *meso*-carbon atoms was 2.434 Å. The deformation angles,  $\alpha$  and  $\beta$ , for  $\mathbf{1}\cdot\text{F}^-$  were calculated to be  $2.45^\circ$  and  $11.3^\circ$ , respectively; this was taken as evidence that the ring strain of **1** around *meso*-carbon atoms was slightly increased upon fluoride anion complexation, an energetic penalty that is presumably overcome through formation of NH–F hydrogen bonds.

Complexation with the fluoride ion was found to stabilize macrocycle **1**. As inferred from high-performance liquid chromatography (HPLC) studies, >98% of **1** (tested as a 3.3 mM dichloromethane solution in the presence TFA (10 mM); Figure S13) disappeared within 10 s to give calix[6]pyrrole **7** along with minor byproducts with higher retention times. In contrast, >70% of **1** remained intact under otherwise identical test conditions.

Boron complexation was also found to stabilize the tripyrrolic macrocycle **1**. Initial deprotonation of the NH protons of **1** using *n*-butyllithium and subsequent treatment with boron tribromide furnished the boron-calix[3]pyrrole **9** in 25% yield (Figure 3C). This stepwise procedure proved necessary to maintain the integrity of **1** since simple treatment with the Lewis acidic boron reagent was found to induce ring-expansion leading to isolation of **8**. A single-crystal X-ray diffraction analysis of **9** revealed a shallow bowl-shaped structure with a trigonal-planar boron(III) center (Figure 3D). Compared to the free-base form **1**, the deformation angles,  $\alpha$  and  $\beta$ , of complex **9** were decreased to  $2.27^\circ$  and  $2.42^\circ$ , respectively. The large decrease seen for the deformation angle  $\beta$  is consistent with macrocyclic ring strain being released upon boron complexation. In fact, boron complex **9** proved stable under the test acidic pyrrole macrocyclization conditions noted above. Specifically, neither ring expansion nor loss of the complexed boron atom was observed.

On the other hand, attempts to prepare **9** under template conditions in the presence of tri(pyrrol-1-yl)borane proved unsuccessful.<sup>32</sup> In the case of boron-subporphyrins heating to  $140\text{--}180^\circ\text{C}$  is necessary to complete the macrocyclization around the boron template.<sup>12,33</sup> Moreover, subporphyrins are stabilized via 14  $\pi$ -electron aromatization; however, the nonaromatic species **9** cannot benefit from such stabilization. Thus, perhaps not surprisingly, only decomposition products were observed when the forcing conditions used to access subporphyrins were attempted in an effort to produce **9**.

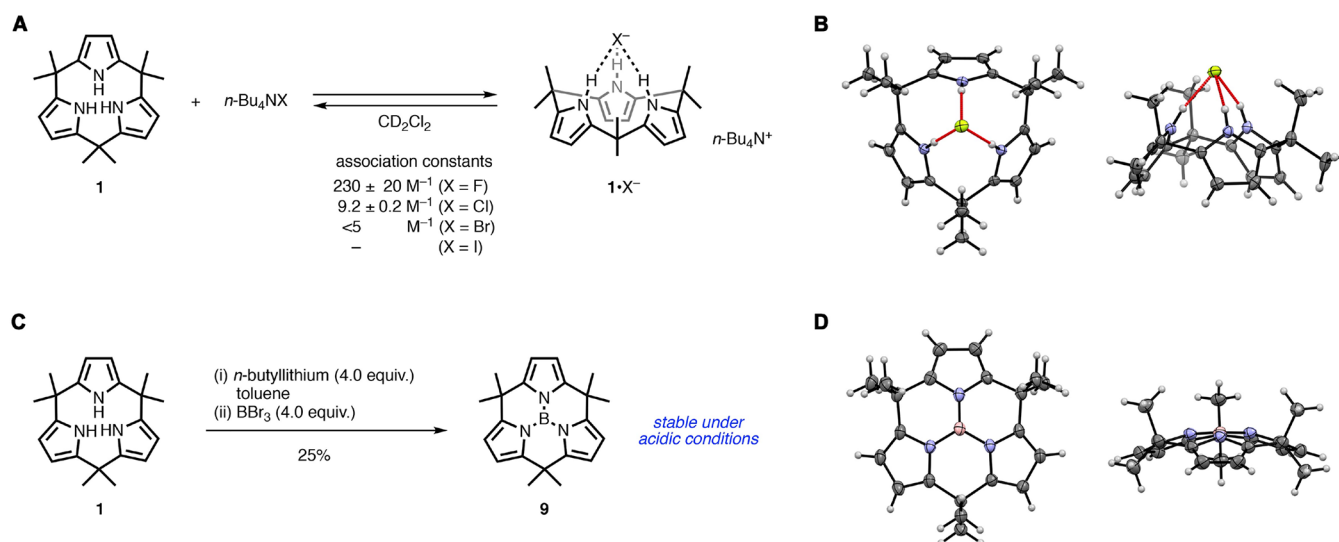


**Figure 3.** (A) Association constants corresponding to the interaction of calix[3]pyrrole **1** with tetrabutylammonium halides in CD<sub>2</sub>Cl<sub>2</sub>. (B) Crystal structure of the fluoride complex, **1**·F<sup>−</sup> (left: top view; right: side view). (C) Synthesis of boron–calix[3]pyrrole complex **9**. As noted in the main text, this species does not undergo a ring-expansion reaction under acidic conditions. (D) Crystal structure of **9** (left: top view; right: side view) shown at the 50% thermal probability level. Hydrogen: white; boron: pink; carbon: gray; nitrogen: light blue; fluorine: yellow.

## CONCLUSION

The present study helps explain the absence of observable tripyrrolic macrocycles during classic porphyrin syntheses. At the reduced porphyrinogen or calix[3]pyrrole-like oxidation level, such species are highly strained and are likely to undergo facile and rapid ring expansion as seen explicitly in the case of calix[3]pyrrole **1**. The present successful synthesis of calix[3]pyrrole and calix[3]furan from cyclic oligoketones was made possible by incorporating a final pyrrole- or furan-forming step that allowed the strain energy to be overcome by formation of an aromatic subunit (pyrrole or furan) under nonequilibrium conditions. The present results lead us to propose that the preparation and subsequent release of macrocyclic ring strain in systems such as **1** and **2** constitute a relatively unexplored approach to achieving C–C bond cleavage and heteroaromatic ring dearomatization. In principle, such transformations could provide access to new porphyrin analogues that might not be accessible through more conventional syntheses.

## ASSOCIATED CONTENT

### Supporting Information

The Supporting Information is available free of charge at <https://pubs.acs.org/doi/10.1021/jacs.1c06331>.

Materials and methods, synthetic procedures, experimental details, computational details, crystallographic data, and NMR spectra for all compounds (PDF)

### Accession Codes

CCDC 2080602–2080609 contain the supplementary crystallographic data for this paper. These data can be obtained free of charge via [www.ccdc.cam.ac.uk/data\\_request/cif](http://www.ccdc.cam.ac.uk/data_request/cif), or by emailing [data\\_request@ccdc.cam.ac.uk](mailto:data_request@ccdc.cam.ac.uk), or by contacting The Cambridge Crystallographic Data Centre, 12 Union Road, Cambridge CB2 1EZ, UK; fax: +44 1223 336033.

## AUTHOR INFORMATION

### Corresponding Authors

Jonathan L. Sessler – Department of Chemistry, The University of Texas at Austin, Austin, Texas 78712-1224,

United States; [orcid.org/0000-0002-9576-1325](https://orcid.org/0000-0002-9576-1325);

Email: [sessler@cm.utexas.edu](mailto:sessler@cm.utexas.edu)

Yasuhide Inokuma – Division of Applied Chemistry, Faculty of Engineering, Hokkaido University, Sapporo, Hokkaido 060-8628, Japan; Institute for Chemical Reaction Design and Discovery (WPI-ICReDD), Hokkaido University, Sapporo, Hokkaido 001-0021, Japan; [orcid.org/0000-0001-6558-3356](https://orcid.org/0000-0001-6558-3356); Email: [inokuma@eng.hokudai.ac.jp](mailto:inokuma@eng.hokudai.ac.jp)

## Authors

Yuya Inaba – Division of Applied Chemistry, Faculty of Engineering, Hokkaido University, Sapporo, Hokkaido 060-8628, Japan

Yu Nomata – Division of Applied Chemistry, Faculty of Engineering, Hokkaido University, Sapporo, Hokkaido 060-8628, Japan

Yuki Ide – Institute for Chemical Reaction Design and Discovery (WPI-ICReDD), Hokkaido University, Sapporo, Hokkaido 001-0021, Japan

Jenny Pirillo – Institute for Chemical Reaction Design and Discovery (WPI-ICReDD), Hokkaido University, Sapporo, Hokkaido 001-0021, Japan; [orcid.org/0000-0002-8866-4279](https://orcid.org/0000-0002-8866-4279)

Yuh Hijikata – Institute for Chemical Reaction Design and Discovery (WPI-ICReDD), Hokkaido University, Sapporo, Hokkaido 001-0021, Japan; [orcid.org/0000-0003-4883-5085](https://orcid.org/0000-0003-4883-5085)

Tomoki Yoneda – Division of Applied Chemistry, Faculty of Engineering, Hokkaido University, Sapporo, Hokkaido 060-8628, Japan; [orcid.org/0000-0002-9804-0240](https://orcid.org/0000-0002-9804-0240)

Atsuhiko Osuka – Department of Chemistry, Graduate School of Science, Kyoto University, Kyoto 606-8502, Japan; [orcid.org/0000-0001-8697-8488](https://orcid.org/0000-0001-8697-8488)

Complete contact information is available at:

<https://pubs.acs.org/doi/10.1021/jacs.1c06331>

## Notes

The authors declare no competing financial interest.

## ACKNOWLEDGMENTS

This work was supported by JSPS Grant-in-Aid for Young Scientists (A) Grant 17H04872, for Challenging Research (Exploratory) Grant 20K21214, and the Asahi Glass Foundation to Y.I. This work was supported by JSPS Grant-in-Aid for Early-Career Scientists Grant 21K14597 and Scientific Research on Innovative Areas “Soft Crystals” to Y.I. The work in Austin was funded by the Robert A. Welch Foundation (F-0018 to J.L.S.).

## REFERENCES

- (1) Horton, P.; Ruban, V. A.; Walters, G. R. Regulation of light harvesting in green plants. *Annu. Rev. Plant Physiol. Plant Mol. Biol.* **1996**, *47*, 655–684.
- (2) Riess, G. J. Oxygen carriers (“blood substitutes”)—raison d’être, chemistry, and some physiology. *Chem. Rev.* **2001**, *101*, 2797–2919.
- (3) Huang, X.; Groves, T. J. Oxygen activation and radical transformations in Heme proteins and metalloporphyrins. *Chem. Rev.* **2018**, *118*, 2491–2553.
- (4) Lu, H.; Zhang, P. X. Catalytic C-H functionalization by metalloporphyrins: recent developments and future directions. *Chem. Soc. Rev.* **2011**, *40*, 1899–1909.
- (5) Bonnett, R. Photosensitizers of the porphyrin and phthalocyanine series for photodynamic therapy. *Chem. Soc. Rev.* **1995**, *24*, 19–33.
- (6) Ethirajan, M.; Chen, Y.; Joshi, P.; Pandey, K. R. The role of porphyrin chemistry in tumor imaging and photodynamic therapy. *Chem. Soc. Rev.* **2011**, *40*, 340–362.
- (7) Li, L.-L.; Diao, E. W.-G. Porphyrin-sensitized solar cells. *Chem. Soc. Rev.* **2013**, *42*, 291–304.
- (8) Rothemund, P. Formation of porphyrins from pyrrole and aldehydes. *J. Am. Chem. Soc.* **1935**, *57*, 2010–2011.
- (9) Kadish, K.; Smith, M. K.; Guillard, R. *The Porphyrin Handbook*; Academic Press: 1999; Vol. 1.
- (10) Saito, S.; Osuka, A. Expanded porphyrins: intriguing structures, electronic properties, and reactivities. *Angew. Chem., Int. Ed.* **2011**, *50*, 4342–4373.
- (11) Meller, A.; Ossko, A. Phthalocyaninartige bor-komplexe. *Monatsh. Chem.* **1972**, *103*, 150–155.
- (12) Inokuma, Y.; Kwon, J. H.; Ahn, T. K.; Yoo, M.-C.; Kim, D.; Osuka, A. Tribenzosubporphyrins: synthesis and characterization. *Angew. Chem., Int. Ed.* **2006**, *45*, 961–964.
- (13) Kobayashi, N.; Takeuchi, Y.; Matsuda, A. meso-Aryl subporphyrins. *Angew. Chem., Int. Ed.* **2007**, *46*, 758–760.
- (14) Claessens, G. C.; González-Rodríguez, D.; Torres, T. Subphthalocyanines: singular nonplanar aromatic compound – synthesis, reactivity, and physical properties. *Chem. Rev.* **2002**, *102*, 835–854.
- (15) Shimizu, S. Recent advances in subporphyrins and triphyrin analogues: contracted porphyrins comprising three pyrrole rings. *Chem. Rev.* **2017**, *117*, 2730–2784.
- (16) Stark, M. W.; Hart, J. G.; Battersby, R. A. Synthetic studies on the proposed spiro intermediate for biosynthesis of the natural porphyrins: Inhibition of cosynthetase. *J. Chem. Soc., Chem. Commun.* **1986**, 465–467.
- (17) Myśliborski, R.; Latos-Grażyński, L.; Szterenber, L.; Lis, T. Subpyrporphyrin—a [14]triphyrin(1.1.1) homologue with an embedded pyridine moiety. *Angew. Chem., Int. Ed.* **2006**, *45*, 3670–3674.
- (18) Kuzuhara, D.; Yamada, H.; Xue, Z.; Okujima, T.; Mori, S.; Shen, Z.; Uno, H. New synthesis of meso-free-[14]triphyrin(2.1.1) by McMurry coupling and its derivatization to Mn(I) and Re(I) complexes. *Chem. Commun.* **2011**, *47*, 722–724.
- (19) Kumar, S. B.; Pati, N. N.; Jose, J. V. K.; Panda, K. P. Synthetic access to calix[3]pyrroles via meso-expansion: hosts with diverse guest chemistry. *Chem. Commun.* **2020**, *56*, 5637–5640.
- (20) Cafeo, G.; Kohnke, F. H.; Parisi, M. F.; Nascone, R. P.; Torre, G. L. L.; Williams, D. J. The elusive  $\beta$ -unsubstituted calix[5]pyrrole finally captured. *Org. Lett.* **2002**, *4*, 2695–2697.
- (21) Cafeo, G.; Kohnke, H. F.; La Torre, L. G.; White, P. J. A.; Williams, J. D. From large furan-based calixarenes to calixpyrroles and calix[n]furan[m]pyrroles: synthesis and structures. *Angew. Chem., Int. Ed.* **2000**, *39*, 1496–1498.
- (22) Uesaka, M.; Saito, Y.; Yoshioka, S.; Domoto, Y.; Fujita, M.; Inokuma, Y. Oligoacetylacetones as shapable carbon chains and their transformation to oligoimines for construction of metal-organic architectures. *Commun. Chem.* **2018**, *1*, 23.
- (23) Manabe, Y.; Uesaka, M.; Yoneda, T.; Inokuma, Y. Two-step transformation of aliphatic polyketones into  $\pi$ -conjugated polyimines. *J. Org. Chem.* **2019**, *84*, 9957–9964.
- (24) Goncalves, S.; Wagner, A.; Mioskowski, C.; Baati, R. Microwave-assisted synthesis of 4-keto-4,5,6,7-tetrahydrobenzofurans. *Tetrahedron Lett.* **2009**, *50*, 274–276.
- (25) Tobe, Y.; Ueda, K.; Kakiuchi, K.; Odaira, Y.; Kai, Y.; Kasai, N. Synthesis, structure and reactivities of [6]paracyclophanes. *Tetrahedron* **1986**, *42*, 1851–1858.
- (26) Baeyer, A. Ueber ein condensationsproduct von pyrrol mit aceton. *Ber. Dtsch. Chem. Ges.* **1886**, *19*, 2184–2185.
- (27) Rothemund, P.; Gage, L. C. Concerning the structure of “acetonepyrrole”. *J. Am. Chem. Soc.* **1955**, *77*, 3340–3342.
- (28) Lindsey, S. J.; Schreiman, C. I.; Hsu, C. H.; Kearney, C. P.; Marguerettaz, M. A. Rothemund and Adler–Longo reactions revisited: synthesis of tetraphenylporphyrins under equilibrium conditions. *J. Org. Chem.* **1987**, *52*, 827–836.
- (29) Taniguchi, R.; Shimizu, S.; Suzuki, M.; Shin, J.-Y.; Furuta, H.; Osuka, A. Ring size selective synthesis of meso-aryl expanded porphyrins. *Tetrahedron Lett.* **2003**, *44*, 2505–2507.
- (30) Ackman, G. R.; Brown, H. W.; Wright, F. G. The condensation of methyl ketones with furan. *J. Org. Chem.* **1955**, *20*, 1147–1158.
- (31) Gale, A. P.; Sessler, L. J.; Král, V.; Lynch, V. Calix[4]pyrroles: old yet new anion-binding agents. *J. Am. Chem. Soc.* **1996**, *118*, 5140–5141.
- (32) Köster, R.; Bellut, H.; Hattori, S. Borverbindungen, XVIII. borstickstoffverbindungen durch aminolyse von triäthyleaminboran und alkyldiboranen. *Liebigs Ann. Chem.* **1968**, *720*, 1–22.
- (33) Inokuma, Y.; Yoon, S. Z.; Kim, D.; Osuka, A. meso-Aryl-substituted subporphyrins: synthesis, structures, and large substituent effects on their electronic properties. *J. Am. Chem. Soc.* **2007**, *129*, 4747–4761.